Highly sensitive cell imaging "Off-on" fluorescent probe for mitochondria and ATP

Priyanka Srivastava, Syed S. Razi, Rashid Ali, Saurabh Srivastav, Satyakam Patnaik, Saripella Srikrishna, Arvind Misra

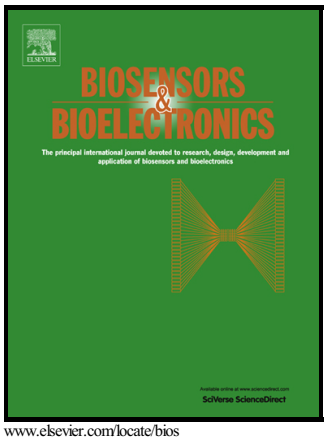

www.elsevier.com/locate/bios

PII: S0956-5663(15)00129-3
DOI: http://dx.doi.org/10.1016/j.bios.2015.02.028
Reference: BIOS7477

To appear in: *Biosensors and Bioelectronic*

Received date: 20 December 2014
Revised date: 15 February 2015
Accepted date: 16 February 2015

Cite this article as: Priyanka Srivastava, Syed S. Razi, Rashid Ali, Saurabh Srivastav, Satyakam Patnaik, Saripella Srikrishna and Arvind Misra, Highly sensitive cell imaging "Off-on" fluorescent probe for mitochondria and ATP, *Biosensors and Bioelectronic,* http://dx.doi.org/10.1016/j.bios.2015.02.028

Highly Sensitive Cell Imaging "*Off-On*" Fluorescent Probe for Mitochondria and ATP

Priyanka Srivastava[†], Syed S. Razi[†], Rashid Ali[†], Saurabh Srivastav[ǁ],

Satyakam Patnaik[§], Saripella Srikrishna[ǁ] and Arvind Misra[†]*

[†] Department of Chemistry, Faculty of Science, Banaras Hindu University, Varanasi – 221005. UP INDIA

Tel.: +91-0542-2307321 ext. 104; +91-0542-6702503 Fax: +91-0542-2368127, 2368175.

Corresponding author E-mail: arvindmisra2003@yahoo.com. amisra@bhu.ac.in

[ǁ] Department of Biochemistry, Faculty of Science, Banaras Hindu University, Varanasi – 221005 UP INDIA

[§] Indian Institute of Toxicology and Research (IITR), Lucknow-226001, UP INDIA

Abstract

A smart *Off-On* molecular scaffold/fluorescent probe **1** has been designed and synthesized. The probe has shown considerable photostability, cell permeability, organelle specificity and selectivity for ATP. The multicolor live cell imaging experiments in HeLa cells showed high selectivity of probe **1** for mitochondria with fluorescence "*turn – On*" response. As a proof of concept and promising prospects for application in biological sciences probe **1** has been utilized to detect ATP sensitively in a partial aqueous medium and intracellularly in HeLa cells. The favorable interaction between triphosphate unit of ATP and piperazine *N* atoms of probe **1** is attributed to synergistic effects of H-bonding and electrostatic interactions that encouraged the CH---π and π→π stacking between anthracene and purine rings. Consequently, the observed enhanced "turn-on" emission and a naked-eye sensitive blue-green color in the medium is attributable to arrest in photoinduced electron transfer (PET) process.

Keywords: Fluorescence, PET, Mitochondria, ATP, Biosensor, Live Cell imaging

1. Introduction

The majority of eukaryotic cells are rich in membrane-enclosed energy producing organelle – mitochondria, which actively participate in several cellular processes such as, cell signaling, cellular differentiation, reactive oxygen species generation and cell death (Mourtada et al., 2013). The mitochondrial dysfunctions directly influence the metabolic activities of cells, and can cause various degenerative and hyperproliferative diseases and cancers (Frantz and Wipf, 2010; Wallace, 1999). Thus, investigations related to structure and function of the mitochondria is of ultimate importance to understanding the respective physiological processes. Recently, researchers have shown the importance of subcellular imaging studies in diagnostics and therapeutics (Yousif et al., 2009) in which application of organelle specific localizable fluorescent probes/scaffolds are more promising, convenient and versatile to monitor biological events with high accuracy and low background (Kurishita et al., 2012; Ojida et al., 2009; Lee et al., 2014). Fluorescence based analytical methods are simple, sensitive, robust, highly specific and enable real-time monitoring of both *in vivo* and *in vitro* bioassays (Valeur, 2002).

Further, in cells the nucleoside polyphosphates (NPPs; like, ATP, GTP, CTP, TTP, UTP) are ubiquitous and play vital role in various cellular events as well as in construction of basic genetic framework of all the life forms (Neelakandan et al., 2006). Particularly, various cellular and metabolic functions require energy in the form of ATP while the extracellular release of ATP and its derivatives also helps to transmit purinergic signal to immunological systems (Xu et al., 2009; 2011). Similarly, GTP is involved in RNA synthesis, citric acid cycle, and acts as an energy source for protein synthesis (Kim et al., 2011).

In last decade, significant efforts have been made to develop selective fluorescent chemosensors to elucidate diverse biological functions in the areas of biochemistry, molecular biology, and clinical diagnostics (Neelakandan et al., 2006; Xu et al., 2009; 2011). However, the number of organelle specific chemosensors is less and needs more attention to understand the spatial dynamics of NPPs in a particular subcellular region as well as for targeted cell imaging studies (Dickinson et al., 2011; Lim et al., 2011; Kim et al., 2011; Ueno et al., 2011; Koide et al., 2011). The molecular receptors and/or chemosensors frequently utilized in NPPs recognition involve hydrogen bonding interactions in aqueous medium however the interference of hydroxyl functions of glycon moieties is a limiting factor (Ramaiah et al., 2010).

In the same perspective, our own research interest is in the direction of development of some new molecular scaffolds/chemosensors for selective detection of biomolecules and ions under important physiological conditions (Misra et al., 2010; Srivastava et al., 2011; 2013; 2014). The main inspiration of the present work is to develop a "smart" molecular scaffolds/fluorescent probe that can easily localize in a specific cellular region particularly, in mitochondria and enable NPPs recognition selectively in the live cells. The bright blue fluorescence of anthracene and wide biological significance of piperazine (Gielen et al., 1999; Guo et al., 2004) unit encouraged us to develop present photoinduced electron transfer (PET) based molecular scaffold/probe **1.** The suitably designed probe containing a piperazine-anthracene core is expected to produce the desired fluorescence response and to have the sensitivity needed to follow mitochondria, mitochondrial pH changes, and NPPs. The success of our probe is ascribed to the fact that it is a PET driven fluorophore for mitochondria targeting and interaction with ATP due to the presence of piperazine subunit. Probe **1** showed good photostability, low cytotoxicity and excellent membrane permeability toward living cells, which could be

successfully applied to monitor intracellular ATP effectively by confocal fluorescence imaging. The uniqueness of this system is that it complexes with ATP through synergistic effects of electrostatic and π—π stacking interactions and signals the event through the changes in emission and NMR spectroscopy techniques. In addition, the intensity changes of **1** as a function of pH in the presence and absence of ATP showed no dramatic spectral change in wide pH range. We envision that this strategy will contribute to improvements in diagnostics and testing wherein mitochondrial pH dynamics are monitored as well as screening potential new mitochondria-targeting drugs.

2. Experimental

2.1. Materials and Methods: For details please see the Supplementary materials**.**

3. Results and Discussion

3.1. Synthesis and photophysical behavior of probe:

The probe **1** was synthesized in good yield by refluxing 1-bezhydrylpiperazine **2** and bischloromethylanthracene **3** in the presence of K_2CO_3. The chemical structure of compounds were characterized by FTIR, ^{1}HNMR, ^{13}CNMR and HRMS spectral data analysis (see the Supplementary materials, Scheme 1 and Fig. S1-S5). The electronic transition spectra of probe **1** (50 μM) showed absorption bands at 395, 374 and 355 nm in HEPES buffer (10 mM; pH 7.0; 70% aqueous ACN) and upon excitation at 376 nm displayed weak emission intensity at 402 and 422 nm (Φ = 0.001) due to photoinduced electron transfer (PET) process. The pH dependent emission spectra of the probe **1** was remained independent in the neutral and alkaline pH 5.5 to 14 however, enhanced emission was observed with a bathochromic shift of 8 nm between pH 5.5 to 4.0 (see the Supplementary materials, Fig. S6a-b). This suggested that probe **1** is well suited to work under physiological pH conditions (pH 7.0) while in acidic medium *N* atoms of piperazine

unit become protonated and led to enhance emission due to restricted PET. Moreover, the photostability of probe **1** was examined by irradiating the probe solution (at 365 nm; in HEPES buffer) under a xenon light source. After excitation at 376 nm, probe **1** showed almost insignificant variation in the emission intensity for 4h thus, suggested the good photostability of probe **1** and ensures the reliability of the fluorescence measurements (see the Supplementary materials, Fig. S7). Furthermore, the emission behavior of probe **1** upon interaction with various probable interferants present in the biological medium such as, metal ions (Na^+, K^+, Ca^{2+}, Zn^{2+}, Co^{2+}, Cu^{2+} , Fe^{2+}, Fe^{3+}, Mg^{2+}, etc), anions (F−, Cl^-, Br^-, I^-, OAc^-, CN^-, ClO_4^-, HSO_4^-, NO_3^-, $P_2O_7^{4-}$ (PPi), PO_4^{3-}), blood plasma protein (BSA) and metabolic thiols (like cysteine) (see the Supplementary materials, Fig. S8) revealed insignificant changes. Thus, it is noteworthy to mention that the present probe **1** can be potentially utilized for organelle specific cell imaging studies and detection of NPPs *in vivo*.

3.2. Cell viability, Specificity and Multicolor Bioimaging studies:

MTT assay was performed in HeLa cells to understand cytotoxic tolerance and cell permeability of different concentration of probe **1** in Krebs-Ringer-HEPES (KRH) buffer (25 mM HEPES, 115 mM NaCl, 5 mM KCl, 1 mM KH_2PO_4, 1.2 mM $MgSO_4$, and 2 mM $CaCl_2$, pH 7.4 ACN/H_2O: 3:7, v/v). MTT assay with respect to control implicated that more than 50% cells were viable up to 40 µM concentration of probe **1** (see the Supplementary materials, Fig. S9). The observed bright blue color fluorescence of incubated HeLa cells under fluorescence microscope (at 380 nm excitation) suggested the excellent cell permeability of probe **1** as well as localization of **1** in the form of foci in the cytosol around the nuclear periphery of HeLa cells while no such bright fluorescence appeared from nuclei (Fig. 1, image A-I).

The observed cell morphology encouraged us to believe that probe has organelle specificity probably, mitochondria and can be potentially explored in targeted bioimaging studies. This we could confirm by performing subcellular colocalization investigations in Hela cells with probe **1** and standard organelle specific biomarkers. The mitochondria tracker monovalent cationic fluorescent biomarker JC-1 (Molecular Probes) is a good tool to investigate the mitochondrial function. The typical difference in the ratio of red/green fluorescence of JC-1 is useful to identify status of cells during the induction of apoptosis (Smiley et al., 1991). Notably, with the rise in mitochondrial membrane potential the fluorescence of JC-1 changes reversibly from a green to red due to dye aggregation (J-aggregates) while cells with low membrane potential show green fluorescence due to excess of monomeric JC-1 (Lemasters and Ramshesh, 2007).

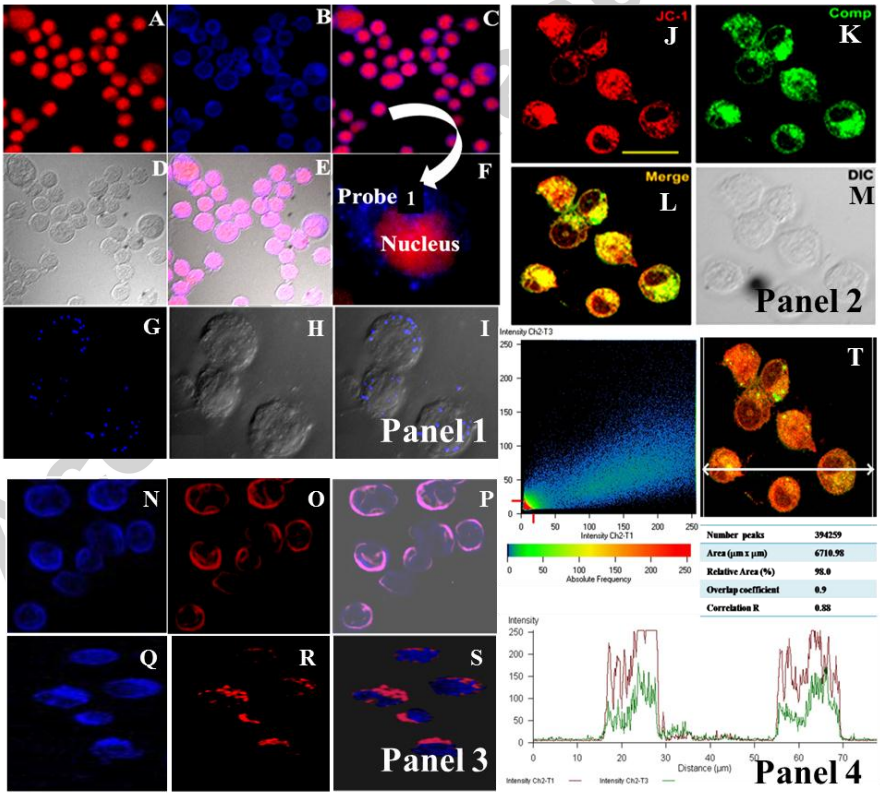

Figure 1

First, we performed colocalization studies to ensure nucleus nonspecificity of probe **1** by

incubating HeLa cells with a nucleus specific dye propidium iodide (PI) (Jones and Kniss, 1987). After proper washing with 1X PBS buffer PI treated HeLa cells were incubated with probe **1** (40 μM) for 1h and then fluorescence images were acquired. Interestingly, the nuclei of the cells appeared in red color (PI, red) (Fig. 1, images A and F) while the blue fluorescence of **1** (Fig. 1, image B) appeared in the cytosol and intense blue color (comp, blue) accumulated at the periphery of the nucleus (Fig. 1, images G-I). The observation clearly suggested the spontaneous localization of probe **1** around the nucleus and in cytosol but not inside the nucleus. Further to have an insight about mitochondria specificity colocalization experiment was performed with probe **1** and dye JC-1 in HeLa cells. The confocal fluorescence microscope images illustrated mitochondria in red (JC1) color while the cells stained with probe **1** appeared in blue (pseudo green) color (Fig. 1, images J and K) respectively. Notably, the superimposed confocal images of HeLa cells clearly suggested about spontaneous localization of **1** and dye JC-1 in the mitochondria. Comparatively, the relative fluorescence intensity correlation plot indicated good affinity (about ~88%) of probe **1** for mitochondria (Fig. 1, image L and T). Next, cell imaging experiments were performed with endoplasmic reticulum and Golgi complex specific biomarkers ER Tracker^{TM} red dye (BODIPY$^{(R)}$ TR Glibenclamide) and Golgin-97 antibody, respectively to ensure selectivity of probe **1** specifically for mitochondria. The incubated cells with the ER Tracker red dye and probe **1** appeared in red and blue colors, respectively (Fig. 1, images N-P) and the colocalized merged confocal images of HeLa cells suggested relatively low binding affinity of probe **1** with endoplasmic reticulum. Similarly, low intensity of probe **1** was observed in colocalization studies with Golgi complex specific dye (Fig. 1, images Q-S and S10). Thus, the multicolor bioimaging experiments provided the concrete evidence about the high organelle specificity of probe **1** to track mitochondria.

3.3. Nucleoside Pyrophosphates (NPPs) Selectivity of Probe 1 in aqueous medium

The dynamics of various functions of mitochondria is difficult to comprehend and is very much dependent on the surrounding pH (Lee et al., 2014). The pH of mitochondrial matrix remains around ~8.0 because the respiratory electron transport process pumps out proton (H^+) across the inner membrane of mitochondria (Abad et al. 2004). So, the medium outside the mitochondrial matrix is acidic and enzyme ATP synthase (H^+-ATP) helps to produce ATP (Voet et al., 2006). A breakdown in this normal homeostasis leads to the production of reactive oxygen species (ROS, such as superoxide etc) that causes apoptosis (Smiley et al., 1991). Similarly, the anomalous aberration in mitochondria proton pump deregulate the Ca^{2+} ion homeostasis (Hajnoczky et al., 2006) that affect dehydrogenase activity associated with the tricarboxylic acid (TCA) cycle, (McCormack et al., 1990) adenine nucleotide translocase (Moreno-Sanchez et al., 1983) as well as of ATP synthase (Yamada and Huzel, 1989).

From these literature supports we envisioned that the observed enhanced emission in HeLa cells is probably due to interaction with ATP and/or protonation of probe **1** due to acidic pH across the inner membrane of mitochondria (Lee et al., 2014). Therefore, we intended to investigate the affinity of probe **1** toward different NPPs (AMP, ADP, ATP, CTP, UTP and GTP) in KRH buffer (10 mM; pH 7.0; 70% aqueous ACN) by absorption and emission spectroscopy. Probe **1** (10 μM) upon interaction with structurally similar nucleoside triphosphates NPPs including AMP and ADP (10 equiv) showed only a marginal change in absorption spectra (blue-shift of ~2-4 nm) (Fig. 2a and S11) however, weak emission intensity of **1** (at 376 nm excitation; $\lambda_{em.}$ = 402 and 422 nm; $\Phi_{\mathbf{5}}$ = 0.001) enhanced significantly, fluorescence "turn-on" (Figure 2a) only in the presence of ATP and the color of solution changed from a dark blue to a fluorescent blue-green (Fig. 2a, images). The high selectivity of probe **1** toward ATP

has been further confirmed by interference studies. It is interesting to mention that the emission intensity of **1**+ATP remained constant upon addition of tested NPPs including AMP and ADP (in excess, 50 equiv) (Fig. 2b).

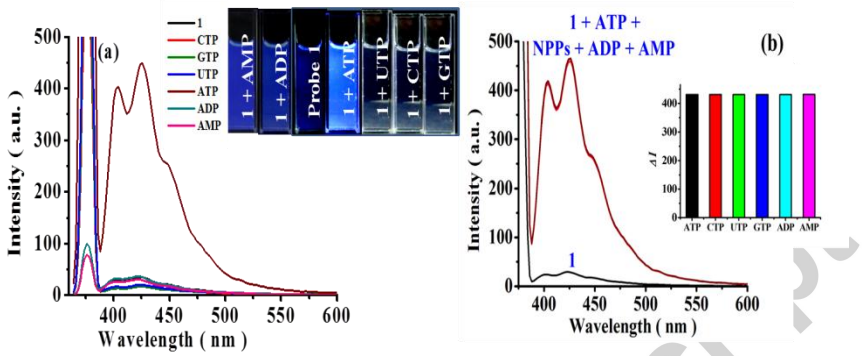

Figure 2

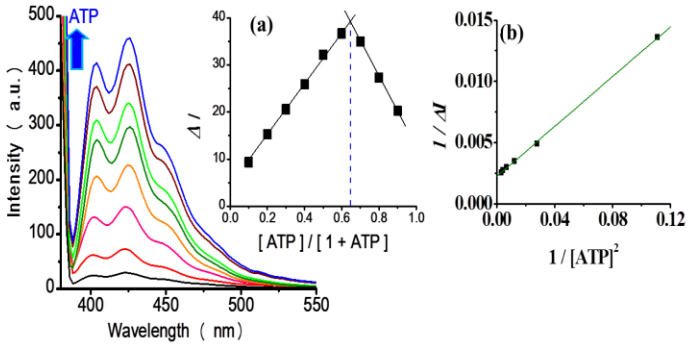

Figure 3

Furthermore, the binding affinity of probe **1** with ATP has been realized through the emission titration experiment. Notably, upon a gradual addition of ATP (0-2.0 equiv) to a solution of probe **1** fluorescence intensity enhanced gradually, (~15 fold) with a red shift of 2-4 nm (Fig. 3) and the estimated quantum yield was increased by ~14 fold (Φ_{5+ATP} = 0.015). Job's plot analysis suggested a 1:2 stoichiometry for an interaction between probe **1** and ATP (Fig. 3a) for which binding constant was estimated by B-H method and found to be 2 x 10^{10} /M^2 (Fig. 3b).

Additionally, to estimate the limit of detection (LOD) a stock solution of **1** was serially diluted from 15.5 to 3.07 μM and emission spectra were acquired (Srivastava et al. 2014). From the linear calibration curve, obtained between the change in relative emission intensities and different concentration of **1** standard deviation was found to be 0.041. Similarly, from the slope of fluorescence curve, obtained between the change in relative fluorescence intensities ($\Delta I = I - I_o$) of **1** (5 μM) and different concentration of ATP calibration sensitivity (m) was estimated and found to be 16.95 (see the Supplementary materials, Fig. S12a-b). Now, applying equation (3) the limit of detection (LOD) of probe **1** to sense ATP was estimated and found to be 0.007 μM (3.69 ppb) which was comparable to other reported methods (Tedsanaa et al., 2013).

3.4. ATP/ADP selectivity of Probe 1

It is reported that except ADP the average concentration of ATP inside the cells is at least 5-fold higher than other NPPs. Therefore, to realize the unique affinity of probe **1** for ATP in the presence of ADP we examined the fluorescence behavior **(**10 samples 10 μM, 3 ml) by varying the ratio of ATP (0-100 μM) and ADP (100-0 μM) such that the total concentration of ATP and ADP remained 100 μM in a 3 mL solution. The emission spectra of probe **1** containing ATP (10 and 20 μM) and ADP (90 and 80 μM) showed fluorescence enhancement while the other gradient systems (containing 30-100 μM of ATP and 70-0 μM of ADP; total concentration = 100 μM) exhibited insignificant change, respectively (see the Supplementary materials, Fig. S13). These results suggested that probe **1** is capable to sense sensitively low concentration (~ 2 equiv) of ATP and effectively even in the environment of ADP.

3.5. Nature of Interaction of Probe 1 with ATP:

In an endeavor to explain the mode of interaction between probe **1** and ATP the ^{1}H NMR titration experiment was performed in DMSO-d_6-D_2O solution (4:1; v/v). ^{1}H NMR spectrum of **1**

(Fig. 4) showed multiplet(s) at δ 8.47 and 7.49 ppm corresponding to anthracene protons (H1, H4, H5, H8 and H2, H3, H6, H7) while benzhydryl protons appeared in the range of δ 7.34-7.14 ppm. The resonances appeared at δ 4.40, 4.20, 2.49 and 2.25 ppm are attributable to H1' ($-CH_2$), H3'' (-CH), H1'' and H2'' ($-CH_2$ of piperazine unit) protons, respectively. Upon addition of ATP (1.0 equiv) to a solution of **1** a set of protons (H1 H4 H5 H8) exhibited upfield shift (Δδ = 0.08 ppm) while other protons (H2 H3 H6 H7) exhibited downfield shift (Δδ = 0.11 ppm) and appeared at δ 8.39 and 7.60 ppm, respectively. Similarly, H1' and H3'' protons shifted downfield to appear at δ 5.06 (Δδ = 0.65 ppm) and δ 4.95 (Δδ = 0.75) ppm, respectively (Fig. 4). Importantly, the piperazine unit protons ($-CH_2$; H1'' and H2'') upon interaction with ATP exhibited considerable downfield shift (Δδ = 1.52 and 1.18 ppm) to appear at δ 4.01 and 3.45 ppm, respectively (see the Supplementary materials, Fig. S14-S17). The net downfield shift clearly suggested about the possible interaction of probe **1** with ATP wherein triphosphate arm of ATP possibly interacted with the *N* atoms of piperazine units. It is important to note that the resonances of a set of 4Hs (H1, H4, H5, H8) of anthracene unit after upfield shift coincides with the resonance of H_a proton of ATP (Fig. 4) and remained in proximity to adenine (purine base) moiety through typical synergistic effect of CH---π and π→π interactions (Xu et al., 2009; 2011; Ramaiah et al., 2010).

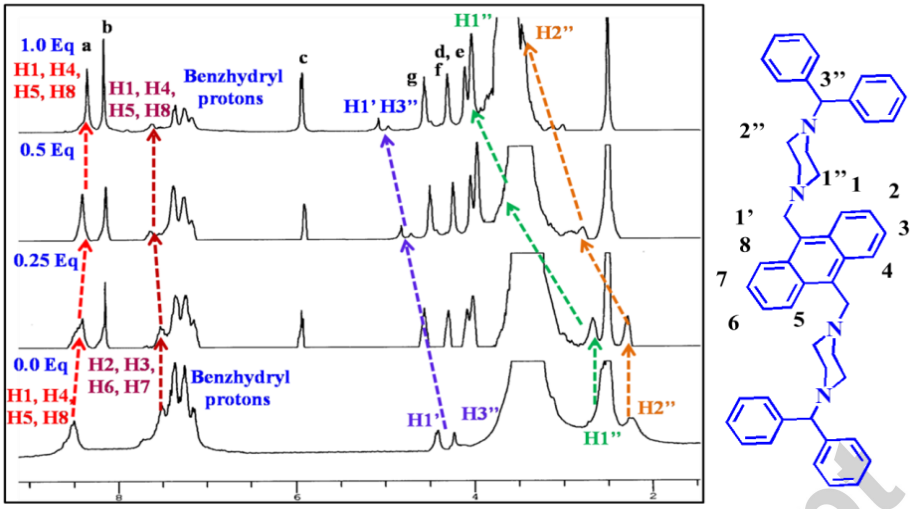

Figure 4

Further to support our hypothesis the ^{1}H and ^{31}P NMR spectra of ATP (disodium salt, Sigma) were acquired before and after the addition of probe **1**. The ^{1}H NMR spectrum of ATP **(**in D_2O) showed resonances assignable to purine ring protons (H_b and H_a) at δ 8.44 and 8.26 ppm while annomeric proton (H_c) appeared at δ 5.97 ppm, respectively. Similarly, the resonances appeared at δ 4.40-4.19 ppm are attributable to protons (H_g, H_f, H_d and H_e) of glycon unit (Xu et al., 2009; 2011). Upon addition of probe **1** (0.25 equiv; in DMSO-d_6) to the solution of ATP upfield shifts were observed corresponding to resonances of H_c ($\Delta\delta$ = 0.005 ppm) and glycon unit protons ($\Delta\delta$ = ~0.005-0.014 ppm) (see the Supplementary materials, Fig. S18a and S19-20) while the purine ring protons (H_a and H_b) marginally shifted downfield ($\Delta\delta$ = ~0.001-0.004 ppm). Similarly, the ^{31}P NMR spectrum of ATP illustrated resonances attributable to α, β and γ phosphorus atoms at δ -3.62, -15.14 and -3.08 ppm, respectively (Jose et al., 2007; Ojida et al., 2002) which upon interaction with **1** became broadened and shifted downfield ($\Delta\delta_{(\alpha \text{ and } \gamma)}$ = 0.5 ppm; $\Delta\delta_{(\beta)}$ = 0.57 ppm) (see the Supplementary materials, Fig. S18b and S21-22).

Moreover, FT-IR spectrum of probe **1** showed characteristic C-N stretching vibration band at 1331, 1261 and 1136 cm^{-1} while in case of ATP bands appeared at 3354, 1104, 1050 and 1257

cm^{-1} are assignable to N-H/O-H, P=O and P-O-H functions, respectively (see the Supplementary materials, Fig. S23-25). Upon interaction with probe **1** significant blue shift occurred in the stretching vibrations of C-N function of **1** and P=O, P-O-H functions of ATP and new bands appeared at 1252, 1132, 1077 and 1132, 1077, 1004 cm^{-1} respectively. Thus, both NMR and FTIR spectral data analysis clearly suggested about the interaction of probe **1** with ATP (1:2 stoichiometry) in which triphosphate chain of two ATP units establishes interaction with *N* atoms of piperazine unit while two adenine (purine base) units with anthracene moiety through CH---π and π→π interactions.

It is noteworthy to mention that probe **1** has shown enhanced emission in HeLa cells, under acidic condition (pH 6.0 to 4.0) as well as upon interaction with ATP but showed insignificant fluorescence response upon interaction with different class of anions including inorganic phosphates (Pi and PPi). Therefore, the week electrostatic interactions due to pyrophosphate chain of ATP are not solely responsible to get enhanced emission. Certainly, the H-bonding and electrostatic interactions of the triphosphate unit of ATP with piperazine *N* atoms of probe **1** synergistically encouraged CH---π and $\pi\rightarrow\pi$ stacking (Xu et al., 2009; 2011) between anthracene and purine rings which in turn arrest the PET and we could observed the naked-eye visual color change as well as enhanced "fluorescence turn-on" response.

3.6. Fluorescence Sensing of ATP in Live cells:

We could able to demonstrate the practical utility of our designed probe **1** to recognize ATP in live cells. In subcellular region particularly, mitochondria a competition between H+ ions, due to acidic medium and ATP is reasonably possible. We could satisfy our this apprehension by performing a model experiment in KRH buffer and emission behavior of probe **1** was examined by the interference of H^+ ions and ATP separately as well as in a solution of **1** containing ATP

and H^+ ions. Interestingly, upon addition of ATP before and after the addition of H^+, the structural emission intensity corresponding to **1**+ATP and/or **1**+H^++ATP remained constant (see the Supplementary materials, Fig. S26). It clearly indicated that the probe is capable to interact with ATP in the absence or presence of excess of H^+ ions in the solution and more or less would behave similarly in the subcellular region. Also, the intensity changes of probe **1** as a function of pH in the presence and absence of ATP showed no dramatic spectral change in wide pH range of 5.5 – 10 within which most biological samples (5.25–8.93) can be tested. Also, in the presence of ATP, probe **1** exhibited good response at lower pH due to the interaction with protonated piperazine unit. As a result, probe **1** could be applied as biosensor to detect ATP in living cells without interference from pH effects. Based on experimental observations a plausible mode of interaction between **1** and ATP has been proposed in figure 5.

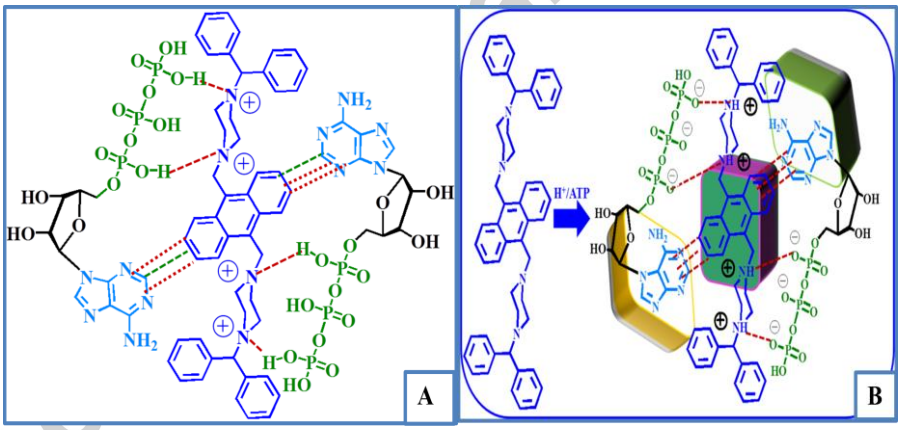

Figure 5

Furthermore, potassium cyanide (KCN) is known to inhibit oxidative phosphorylation in mitochondria (de-energization) under glucose starvation condition (Kurishita et al., 2012; Ojida et al., 2009; Lemasters and Ramshesh, 2007). Therefore, to accomplish the actual sensing ability of **1** an attempt has been made to acquire live cell images upon interaction with additional

supplement of extracellular ATP (10 equiv) in HeLa cells and in the presence/absence of glucose and KCN (0.1 mM). Notably, figure 6 shows that in the presence of glucose HeLa cells fluoresce blue on spontaneous localization with **1** (image A), **1**+KCN (image B) and **1**+ATP (image C). However, under the glucose starvation condition the fluorescence blue color of HeLa cells with **1**+KCN (image D) diminished after 10 min (image E). Thus, suggested about high affinity of probe **1** for ATP in living cells. This is because when ATP was supplemented from outside in the HeLa cells (**1**+KCN+ATP; image F) the blue fluorescence was remained persistent. The observation further suggested that under glucose starvation condition when KCN is added to the HeLa cells the production of ATP decreased while in the presence of glucose formation of ATP remained unhindered. Thus the observed persistent blue fluorescence of probe **1** is compensated by ATP synthesis and KCN has not affected the concentration of external ATP as well as inside the cell.

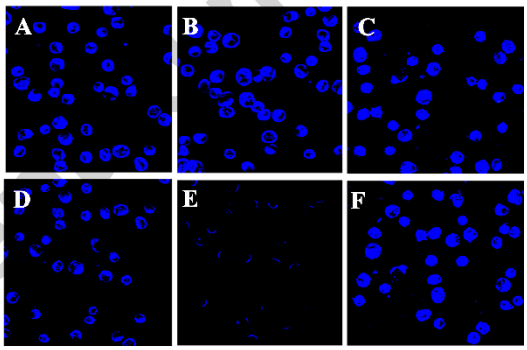

Figure 6

4. Conclusion

In summary, we have successfully deigned a rational organelle specific fluorescence probe that enables selective recognition of ATP in live cell and in aqueous medium. The multicolor live cell imaging experiments with organelle specific biomarkers like, JC-1 (mitochondria), ER tracker red (Endoplasmic reticulum) and Golgin-97 (Golgi complex) have shown relatively high

selectivity of probe **1** for mitochondria. Moreover, the aqueous medium studies favor the interaction of triphosphate unit of ATP with piperazine *N* atoms of probe **1** through H-bonding and electrostatic interactions that synergistically enhance CH---π and π→π stacking interactions between anthracene and purine rings. Consequently, the enhanced "turn-on" emission was observed due to the restricted PET in which a naked-eye sensitive blue-green color appeared in the medium. We believe that the present findings have significance in the progress of cellular bioimaging techniques and will enable the application of self-localizable fluorescent probes/biosensors in elucidating important biological events, metabolic processes and to gain important information about the dynamics of nucleoside pyrophosphates *in vivo*. Our ongoing research activities are engaged in this direction and trying to develop some efficient organelle specific cell imaging fluorescence probes to uncover such important issues.

Acknowledgements

Authors are thankful to Council of Scientific and Industrial Research (CSIR), New Delhi for financial support and senior research fellowships (to PS, SSR and RA) to carry out research work.

References

Abad, M. F. C., Di Benedetto, G., Magalhaes, P. J., Filippin, L., and Pozzan, T. 2004. J. Biol. Chem. 279, 11521−11529.

Dickinson, B. C., Tang, Y., Chang, Z., and Chang, C. J. 2011. Chem. Biol. 18, 943-948.

Frantz, M. C., and Wipf, P. 2010. 51, 462-475.

Gielen, M., Boualam, M., Biesemans, M., Mahieu, B.,Willem, R. 1992. Heterocyclics. 34, 549-559.

Guo, C. C., Tong, R. B., and Li, K. L. 2004. Bioorg. Med. Chem. 12, 2469-2475.

Hajnoczky, G., Csordas, G., Das, S., Garcia-Perez, C., Saotome, M., Sinha Roy, S., Yi, M. 2006. Cell Calcium 40, 553−560.

Jones, K. H., and Kniss, D. A., 1987. J. Histochem Cytochem. 35, 123-125.

Jose, D. A., Mishra, S., Ghosh, A., Shrivastav, A., Mishra, S. K., and Das, A., 2007. Org. Lett. 9, 1979-1982.

Kim, H. N., Moon, J. H., Kim, S. K., Kwon, J. Y., Jang, Y. J., Lee, J. Y., and Yoon, J. 2011. J. Org. Chem. 76, 3805-3811.

Koide, Y., Urano, Y., Hanaoka, K., Terai, T., and Nagano, T., 2011. J. Am. Chem. Soc. 133, 5680–5682.

Kurishita, Y., Kohira, T., Ojida, A., and Hamachi, I. 2012. J. Am. Chem. Soc. 134, 18779−18789.

Lee, M. H., Park, N., Yi, C., Han, J. H., Hong, J. H., Kim, K. P., Kang, D. H., Sessler, J. L. Kang, C., and Kim, J. S. 2014. J. Am. Chem. Soc. 136, 14136–14142.

Lemasters J. J., and Ramshesh V. K., 2007. Methods Cell Biol. 80, 283–295.

Lim, C. S., Masanta, G., Kim, H. J., Han, J. H., Kim, H. M., and Cho, B. R. 2011. J. Am. Chem. Soc. 133, 11132-11135.

Misra, A., and Shahid, M.2010. J. Phys. Chem. C. 114, 16726-16739.

McCormack, J. G., Halestrap, A. P., and Denton, R. M. 1990. Physiol. Rev. 70, 391−425.

Moreno-Sanchez, R. 1983. Biochim. Biophys. Acta. 724, 278−285.

Mourtada, R., Fonseca, S. B., Wisnovsky, S. P., Pereira, M. P., Wang, X., Hurren, R., Parfitt, J., Larsen, L., Smith, R. A. J., Murphy, M. P., Schimmer, A. D., and Kelley, S. O. 2013. PLoS One 8, e60253.

Neelakandan, P. P., Hariharan, M., and Ramaiah, D. 2006. J. Am. Chem. Soc. 128, 11334-

11335.

Ojida, A., Sakamoto, T., Inoue, M., Fujishima, S-H., Lippens, G., and Hamachi, I., 2009. J. Am. Chem. Soc.131, 6543–6548.

Ojida, A., Park, S.-K., Mito-oka, Y., Hamachi, I. 2002.Tetrahedron Lett. 43, 6193-6195.

Ramaiah, D., Neelakandan, P. P., Nair, A. K., and Avirah, R. R. 2010. Chem. Soc. Rev. 39, 4158-4168.

Smiley, S. T., Reers, M., Mottola-Hartshorn, C., Lin, M., Chen, A., Smith, T. W., Steele, G. D., Jr., and Chen, L. B. 1991.Proc. Natl. Acad. Sci. USA 88, 3671–3675.

Srivastava, P., Shahid, M., and Misra, A. 2011. Org. Biomol. Chem. 9, 5051-5055.

Srivastava, P., Ali, R., Razi, S. S., Shahid, M., and Misra, A. 2013. Sens. Actuators, B. 181, 584-595.

Srivastava, P., Razi, S. S., Ali, R., Gupta, R. C., Yadav, S. S., Narayan, G., and Misra, A. 2014. Anal. Chem. 86, 8693−8699.

Tedsanaa, W., Tuntulanib, T., and Ngeontaea, W., 2013. Anal. Chim. Acta. 783, 65– 73.

Ueno, T., Komatsu, T., and Nagano, T., 2011. J. Am. Chem. Soc. 133, 14157–14159.

Valeur, B. 2002. Molecular Fluorescence: Principles and Applications, Wiley-VCH, New York.

Voet, D., Judith, G. V., and Charlotte, W. P., 2006. Fundamentals of Biochemistry, 2nd ed.; John Wiley & Sons, Inc.: New York.

Wallace, D. C. 1999. Science 283, 1482-1488.

Xu, Z., Song, N. R., Moon, Lee, J. H. and Yoon, J. 2011. Org. Biomol. Chem. 9, 8340-8345.

Xu, Z., Singh, N. J.; Lim, J., Pan, J., Kim, H. N. Park, S., Kim, K. S., and Yoon, J. 2009. J. Am. Chem. Soc. 131, 15528-15533.

Yamada, E. W., and Huzel, N. J., 1989. Biochemistry 28, 9714−9718.

Yousif, L. F., Stewart, K. M., and Kelley, S. O. 2009. Chem. Bio. Chem. 10, 1939-1950.

FIGURE CAPTIONS

Fig. 1. Fluorescence images of HeLa cells stained with; Panel 1: (A) propidium iodide (PI), (B) probe **1,** (C) colocalization with PI and **1,** (D) DIC image, (E) Merged images of A, B and D, (F, G, H, and I) magnified views, Panel 2: (J) JC-1 (red), (K) probe **1** (pseudo green), (L) merged and (M) DIC, Panel 3: (N, Q) probe **1**, (O) BODIPY$^{(R)}$ TR Glibenclamide, (R) Golgin-97 and (P, S) merged, Panel 4: Confocal fluorescence spectroscopy based fluorescence image intensity correlation between dye JC-1 and probe **1**.

Fig. 2. (a) Change in intensity of **1** and (b) **1**+ATP upon interaction with NTPs; (50 equiv) in KRH buffer. Insets: change in color of **1** under UV light at 365 nm. Bar diagram of interference studies.

Fig. 3. Emission titration spectra of **1** upon addition of ATP (0-2 equiv) in KRH buffer. (a) Job's and (b) B-H plots of **1** with ATP.

Fig. 4. Partial ^{1}H NMR titration spectra of **1** upon addition of ATP (0-1.0 equiv) in DMSO-d^6/D_2O (4:1; v/v).

Fig. 5. Plausible mode of interaction between probe **1** and H^+/ATP.

Fig. 6. Confocal fluorescence images of HeLa cells upon spontaneous localization of (A) probe **1**; (B) **1** + KCN in the presence of glucose; (C) **1**+ATP; (D) **1**+KCN (E) **1**+KCN after 10 min under glucose starvation condition and (F) **1**+KCN+ATP under glucose starvation condition.

Highlights

- A smart molecular scaffold/fluorescent probe exhibiting fluorescence *Off-On* response.
- Multicolor live cell imaging shows selectivity of probe for mitochondria.
- The probe shows interaction with ATP due to synergistic effects of H-bonding, electrostatic and CH---π and π→π interactions.
- The enhanced "turn-on" emission and a naked-eye sensitive blue-green color in the medium are attributable to arrest in photoinduced electron transfer (PET) process.
- The work has significance in the area of cellular bioimaging techniques and will be helpful in elucidating important biological events and dynamics of nucleoside pyrophosphates *in vivo*.

Graphical Abstract